

# Formation of Nano-Structures under High Pressure

J. Chen, P. Raterron, D. Weidner and M. Vaughan

Center for High Pressure Research, Mineral Physics Institute, State University of New York at Stony Brook, Stony Brook, NY

## Introduction

Behavior of materials at nanoscale (1 to 100 nm) size exhibits a novel and significant change in magnetism, catalysis, optics, electricity and mechanics compared to the behavior of isolated molecules (~1 nm) or of bulk materials. The new behavior at the nanoscale is not necessarily predictable from that observed at large scales. The most important changes in behavior are caused not by order of magnitude size reduction, but by newly observed phenomena intrinsic to or becoming predominant at the nanoscale. These phenomena include size confinement, predominance of interfacial phenomena and quantum effects. Once it becomes possible to control feature size, it will also become possible to enhance material properties and device functions. Reduction of the dimensions of structures down to the nanoscale enhances the unique properties of many materials, such as carbon nanotubes, quantum wires and dots, thin films, DNA-based structures, and laser emitters.

Formation of nanoscale particles has thus become one of the most fundamental elements of nanoscience. In the past decade, several new techniques have been developed to synthesize nanoparticles in addition to mechanical alloying (a high-energy ball milling process), for example, a) *the aerosol technique* [Wu et al., 1993], a gas-to-particle conversion process; b) *soft lithography* [Chou et al., 1996; Kim et al., 1995; Xia et al., 1997; Zhao et al., 1996], a process using transparent, elastomeric polydimethylsiloxane (PDMS) "stamps" with patterned relief on the surface to generate nanosize features; and c) *self-assembly processes* [Sarikaya and Aksay, 1994; Wang et al., 1997], a process to produce ceramics with nanostructural patterns through self-assembly of surfactants or macromolecules templates. Here we report observations of the nanostructure formation in oxides at high pressures by using in-situ x-ray diffraction.

### 1. Grain size measurement by x-ray diffraction

Grain size of samples is measured by monitoring the peak broadening of energy dispersive *in situ* x-ray diffraction during compression. Peak broadening is generally caused by either strain or small grain size and can be described by [Klug and Alexander, 1974; Warren, 1989]

$$B^2 = B_s^2 + B_d^2 \quad (1)$$

where  $B$  represents the line breadth (refers to full width at half maximum, FWHM, of a gaussian profile in our experiments), subscripts  $s$  and  $d$  represent the contribution of grain size and crystal distortion, respectively. In the case of energy dispersive diffraction the  $B_s$  and  $B_d$  can be expressed as [Gerward et al., 1976]

$$B_s = \frac{K(\frac{1}{2}hc)}{P \sin \theta_0} \quad (2)$$

$$B_d = 2eE \quad (3)$$

where  $K$  is the Scherrer constant (usually assumed to be 0.9),  $h$  is Planck's constant,  $c$  is the velocity of light,  $P$  is the average grain size,  $2\theta_0$  is the fixed scattering angle,  $e$  is the maximum elastic strain, and  $E$  is the x-ray photon energy. Average grain size (diffraction domains) is the only energy independent contribution to the diffraction peak broadening (i.e. Eq. 1). Therefore, the sample grain size can be derived for a given diffraction pattern by linearly fitting the square of the experimental peak width,  $B^2$ , to the square of the photon energy,  $E^2$ . This technique, however, only applies to grain size smaller than 200 nm because, for larger grain size, the energy independent term (grain size contribution) in Eq. 1 is almost zero (negligible).

To account for instrumental broadening,  $B_i$ , equation 1 can be modified as [Warren, 1989]

$$B^2 - B_i^2 = B_s^2 + B_d^2 \quad (4)$$

A stress-free standard material for x-ray diffraction with ideal grain size (~1 $\mu$ m) can be used to sample the instrumental broadening before each experiment. If peak broadening for the diffraction standard is measured to be  $B_o$ , the energy-independent term (i.e. Eq. 2) and therefore the average grain size ( $P$ ) will be derived by plotting  $B^2 - B_o^2$  versus  $E^2$ .

### 2. Experimental

The experiments are carried out by using a cubic-type multi-anvil press (SAM85) [Weidner et al., 1992] at the superconductor wiggler beamline X17B of the National Synchrotron Light Source (NSLS). The high

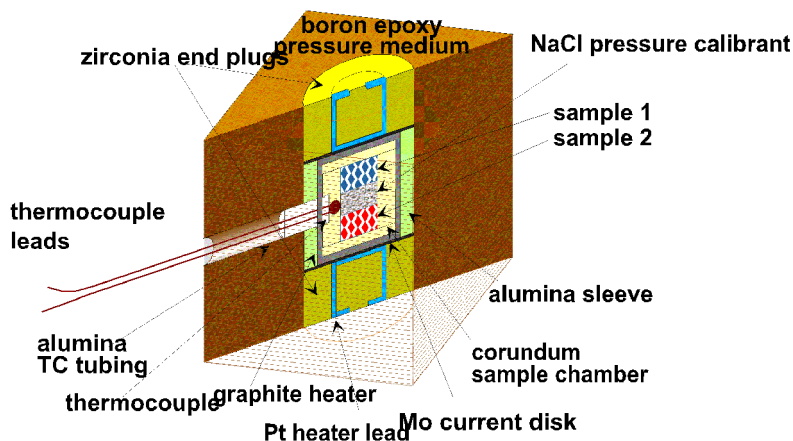


**Figure 1.** The high pressure cell assembly used at the X17B beamline.

pressure cell assembly is shown in Figure 1. The pressure medium is made of a mixture of amorphous boron and epoxy (4:1). The internal heater is a sleeve of amorphous carbon. A W5%Re-W23%Re thermocouple is used to measure the temperature at different pressures (with no correction for pressure dependence).

A high-energy synchrotron radiation beam emitted from the wiggler is defined to 0.2 mm x 0.1mm in size by two incident slits before entering the pressure medium. Diffracted x-rays from the sample are collimated by two sets of receiving slits at a fixed  $2\theta$  angle to the incident beam. A germanium solid state detector (SSD) is used to collect an energy dispersive diffraction pattern.

In the present study, starting samples are  $\text{Fe}_2\text{SiO}_4$  (fayalite) and  $(\text{Mg}_{0.9}\text{Fe}_{0.1})_2\text{SiO}_4$  loose powders with an average grain size of 1  $\mu\text{m}$ . Samples are loaded into cylindrical capsules together with a layer of pressure calibrant (NaCl). Sample pressure is determined by referring the measured unit cell volume of NaCl, through x-ray diffraction, to Decker's scale [Decker, 1971]. Samples are first compressed at room temperature and then heated at high pressure. X-ray diffraction patterns of the sample and pressure calibrant are recorded during the compression and heating.

### 3. Result and Discussion

#### a. $\text{Fe}_2\text{SiO}_4$

Instrumental peak broadening is sampled by measuring the diffraction peak width of a standard material (powdered NaCl) at ambient (room T and P) condition. Figure 2 shows a plot of the peak width ( $\text{FWHM}^2$ ) versus the photon energy ( $E^2$ ) in the diffraction pattern of NaCl. Data from a  $\text{Fe}_2\text{SiO}_4$  sample at ambient condition and high pressure (7 GPa)-room temperature are also plotted in Figure 2. Lines represent linear fitting to the experimental data. At ambient condition, fittings to

the data of sample and NaCl yield the same intercept on the FWHM axis, indicating both of the materials have fairly large grain size and are sampling the instrumental peak broadening. The slightly greater slope of the linear fitting for the sample indicates that there exists measurable grinding residual stress in the sample. At high pressure, diffraction data from the sample yield a fitting that exhibits significant increases of both intercept and slope with respect to those at ambient condition. The average grain size and strain of the sample at high pressures can be derived from the fitting parameters and Eqs. 2, 3 and 4.

Figure 3 shows the derived average grain size and shear stress of the sample as a function of pressure. The grain size decreases significantly while the shear stress builds up quickly upon compression. The grain-size reduction reaches a plateau of about 20 nm at 5 GPa, and no further size reduction is observed beyond this pressure up to 7GPa. On the other hand, the shear stress increases dramatically during the initial loading (Region I in Figure 3), then the stress increases at a slower rate with further loading (Region II). Above 5 GPa, the stress remains almost constant (Region III). These observations indicate that the quickly built-up stresses induce significant cataclasis grain size reduction in the powder sample. Upon further compression the stress reaches the yield strength of the sample and it begins to deform plastically. The measured stress, therefore, represents strength of the sample at the given experimental pres-

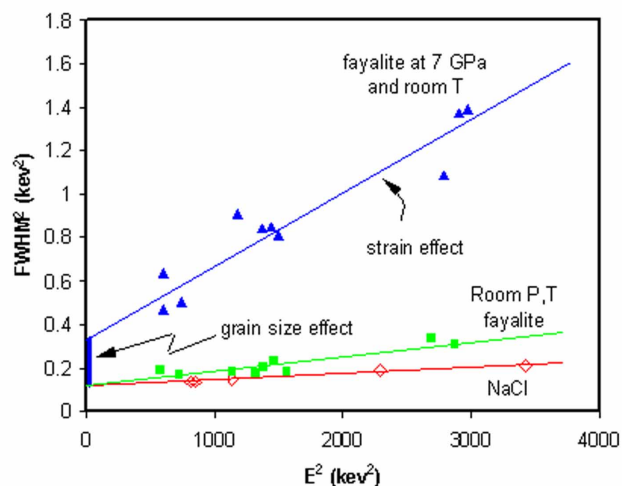


**Figure 2.** Square of peak width ( $\text{FWHM}^2$ ) versus Square of photon energy ( $E^2$ ) in the diffraction patterns of NaCl and  $\text{Fe}_2\text{SiO}_4$  (fayalite) at ambient condition, and  $\text{Fe}_2\text{SiO}_4$  at high pressure (7 GPa)-room temperature.

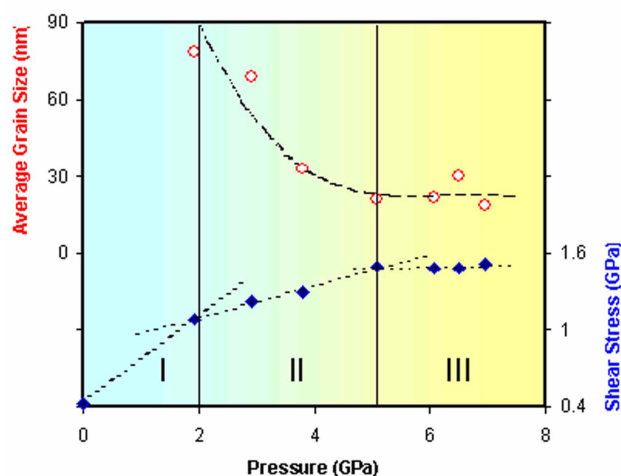


**Figure 3.** Average grain size (circles) and shear stress (diamonds) of the  $Fe_2SiO_4$  sample during cold compression

sure and temperature (Region II). As the porous powder sample is compacted and densified through the cataclasis and deformation, all the initial void spaces between the grains close up. The stress in the sample, therefore, reaches its maximum value, and begins to remain constant. Consequently, the cataclasis process stops.

Upon heating at high pressure, the sample starts to recrystallize and the grain size increases as a function of temperature. Figure 4 shows such an increase in grain size measured by x-ray diffraction peak broadening. At 450 °C, the sample completes a phase transition from an olivine (orthorhombic) structure to a spinel (cubic) structure. The measured grain size of the spinel

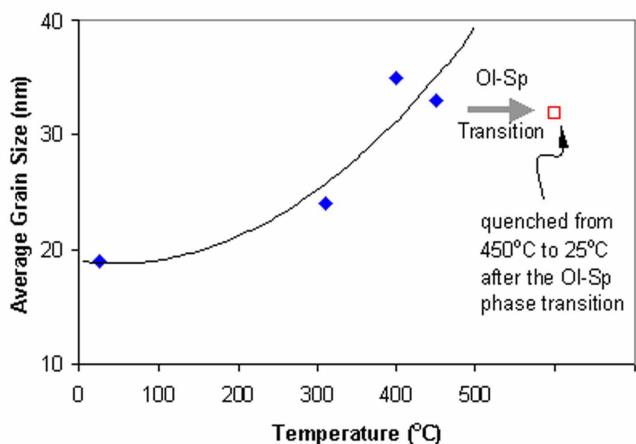


**Figure 4.** Grain size change of  $Fe_2SiO_4$  sample during heating at high pressure.

phase after quenching is the same as that of the olivine phase before the transition (Figure 4), which is consistent with the pseudomartensitic transformation mechanism observed in this transition [Chen *et al.*, 2001a; Chen *et al.*, 2001b].

The recovered sample is examined by using transmission electron microscopy (TEM). Figure 5 shows a bright field TEM micrograph of the sample and a corresponding electron diffraction pattern, obtained from a 0.4- $\mu$ m-diameter area (insert). The sample now exhibits nanometric spinel grains (less than 50 nm in diameter) with an average grain size of about 30 nm in full agreement with the x-ray diffraction measurement (see Figure 3). The spinel grains are randomly oriented as evidenced by the homogeneous Debye rings of the diffraction pattern. The excellent agreement between the TEM and x-ray diffraction data gives us confidence in the x-ray peak broadening method for determining, in situ, the average grain size of high pressure samples.

### b. $(Mg_{0.9}Fe_{0.1})_2SiO_4$

The compression-induced formation of nanostructure is also observed in  $(Mg_{0.9}Fe_{0.1})_2SiO_4$ . Two experiments similar to those described above were carried out for this substance. Two loose powder samples were first cold compressed to 9 GPa. Upon cold compression, the grain size was significantly reduced. Shear stresses in the samples increased first linearly with pressure up to about 2.7GPa, then remained constant while the samples deformed plastically up to 9 GPa. The temperature was then increased in steps ( $\sim 3^\circ$ C/sec) up to 400°C for sample SC1 and 625°C for sample SC2. Stress relaxation was observed in the samples during heating. Figure 6 shows the differential stress (twice the shear stress) versus time as the samples are heated. The x-ray diffraction also indicates that both samples exhibited very fine (nanometric) grain size after cold compression. The grain size then slightly increased with increasing temperature, to reach about 40 nm at 400°C. After the observed 625°C-stress drop, grain size could not be accurately measured by the x-ray diffraction peak broadening in the sample (typically  $> 200$  nm), which suggests that the observed stress drop is accompanied by a rapid grain growth in the materials.

Figure 7 is a dark field TEM micrograph of the recovered sample after the 400°C annealing, showing one grain of the starting olivine powder. A corresponding electron diffraction pattern is shown in the insert. The olivine grain, which was initially about 2-3  $\mu$ m in size, now exhibits nanometric sub-domains resulting from nano-cracking during cold compression, probably along the olivine {010} and {100} cleavage planes, as was previously reported in  $Mg_2SiO_4$  forsterite at high pressure [Brearley *et al.*, 1992]. Similar nanometric aggre-

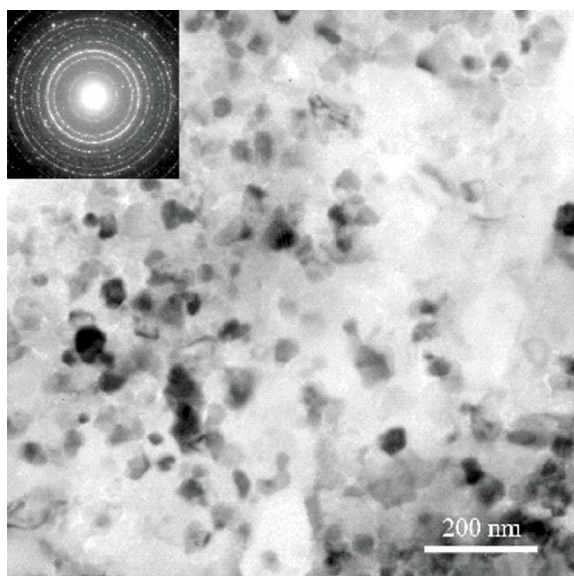


**Figure 5.** Bright field TEM micrograph of the recovered  $\text{Fe}_2\text{SiO}_4$  sample. Insert: electron diffraction pattern, obtained from a  $0.4\text{-}\mu\text{m}$ -diameter area.

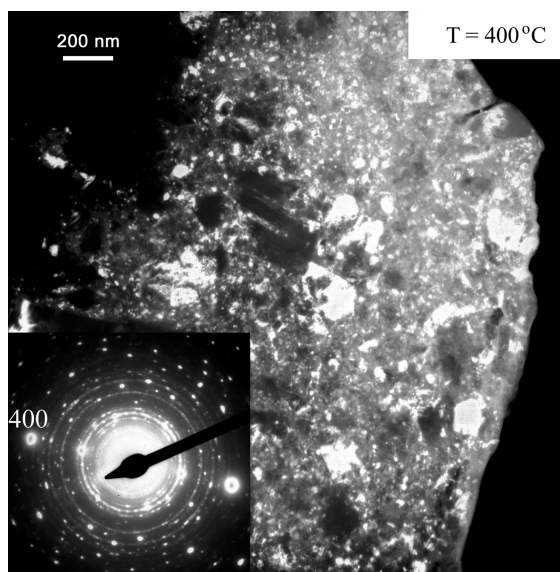


**Figure 7.** Dark field TEM micrograph of the recovered sample from 9 GPa and  $400^\circ\text{C}$ .

gates were also observed in natural olivine from shocked meteorites [Joreau *et al.*, 1998], which experienced a high pressure, low temperature regime immediately following the shock front. In Figure 7, while the starting single crystal diffraction pattern is still visible in the insert, the Debye rings corresponding to the crystallographic disoriented sub-domains are also visible. The size of the sub-domains range from between a few nm to a few hundred nm, most of the material exhibiting a grain size in the 50 nm range, which is consistent with x-ray diffraction grain size measurements. Conversely, no grain smaller than typically 150

nm were observed by TEM in the sample quenched at  $625^\circ\text{C}$ . This indicates that the  $625^\circ\text{C}$  stress drop is accompanied by extensive grain growth.

#### 4. Conclusion

Formation of nanostructure in  $\text{Fe}_2\text{SiO}_4$  and  $(\text{Mg}_{0.9}\text{Fe}_{0.1})_2\text{SiO}_4$  has been observed by using high pressure *in situ* x-ray diffraction and TEM. The experiments also demonstrate that *in situ* x-ray diffraction is a useful method for diagnosing nanomaterial syntheses. Some materials may also form nanostructure under high pressures due to microscopic stresses.

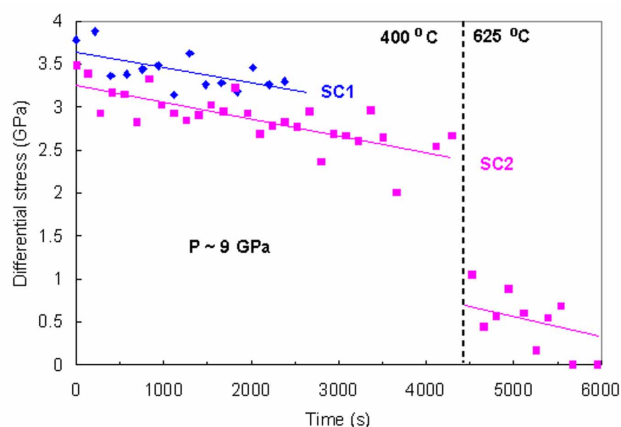


**Figure 6.** Stress relaxation in the  $(\text{Mg}_{0.9}\text{Fe}_{0.1})_2\text{SiO}_4$  samples at  $400^\circ\text{C}$  and  $625^\circ\text{C}$ . SC1 (blue) and SC2 (purple) indicate different experiments.

#### References

- Brearley, A.J., D.C. Rubie, and E. Ito, Mechanisms of the transformations between the  $\alpha$ ,  $\beta$  and  $\gamma$  polymorphs of  $\text{Mg}_2\text{SiO}_4$  at 15 GPa, *Physics and Chemistry of Minerals*, 18, 343 - 358, 1992.
- Chen, J., D.J. Weidner, J.B. Parise, M.T. Vaughan, and P. Raterron, Observation of cation reordering during the olivine-spinel transition in fayalite by *in situ* synchrotron x-ray diffraction at high pressure and temperature, *Physical Review Letters*, 86 (18), 4072 - 4075, 2001a.
- Chen, J., D.J. Weidner, J.B. Parise, M.T. Vaughan, and P. Raterron, Pseudomartensitic Phase Transformation, *NLS Newsletter*, July, 1 - 4, 2001b.
- Chou, S.Y., P.R. Krauss, and P.J. Renstrom, Imprint lithography with 25-nanometer resolution, *Science*, 272, 85 - 87, 1996.
- Decker, D.L., High pressure equation of state for NaCl, KCl, and CsCl, *Journal of Applied Physics*, 42 (8), 3239 - 3244, 1971.

- Gerward, L., S. Morup, and H. Topsoe, Particle size and strain broadening in energy-dispersive x-ray powder patterns, *J. Appl. Phys.*, **47**, 822-825, 1976.
- Joreau, P., H. Lerous, and J.-C. Doukhan, A transmission electron microscope investigation of shock metamorphism in olivine from the Ilafegh 013 chondrite, *Meteoritics & planetary Science*, **32**, 309 - 316, 1998.
- Kim, E., Y. Xia, and G.M. Whitesides, Polymeric Microstructures Formed by Moulding in Capillaries, *Nature*, **376**, 581-584, 1995.
- Klug, H.P., and L.E. Alexander, *X-ray Diffraction Procedures*, Wiley, New York, 1974.
- Sarikaya, M., and I.A. Aksay, *Design and processing of materials by biomimicking*, Am. Inst. Physics, New York, 1994.
- Wang, D., S.G. Thomas, K.L. Wang, Y. Xia, and G.M. Whitesides, Nanometer scale patterning and pattern transfer on amorphous Si, crystalline Si, and SiO<sub>2</sub> surfaces using self-assembled monolayers, *Appl. Phys. Lett.*, **70**, 1593, 1997.
- Warren, B., *X-ray Diffraction*, Addison-Wesley, London, 1989.
- Weidner, D.J., M.T. Vaughan, J. Ko, Y. Wang, X. Liu, A. Yeganeh-Haeri, R.E. Pacalo, and Y. Zhao, Characterization of stress, pressure, and temperature in SAM85, a DIA type high pressure apparatus., in *High pressure research: Application to Earth and planetary sciences*, edited by Y. Synono, and M.H. Manghnani, pp. 13 - 17, Terra Scientific Publishing Company / AGU, Tokyo / Washington, D.C., 1992.
- Wu, M.K., R.S. Windeler, C.K. Steiner, T. Bors, and S.K. Friedlander., Controlled synthesis of nanosized particles by aerosol processes, *Aerosol Sci. Technol.*, **19**, 527, 1993.
- Xia, Y., J.J. McClelland, R. Gupta, D. Qin, X.-M. Zhao, L.L. Sohn, R. Celotta, and G.M. Whitesides, Replica Molding Using Organic Polymers: A Step Toward Nanomanufacturing, *Advanced Materials*, **9**, 147 - 149, 1997.
- Zhao, X.-M., Y. Xia, and G.M. Whitesides, Fabrication of Three-Dimensional Microstructures: Microtransfer Molding, *Advanced Materials*, **8**, 837 - 840, 1996.